Precipitation mediates sap flux sensitivity to evaporative demand in the neotropics

Charlotte Grossiord, Bradley Christoffersen, Aura Alonso-Rodríguez, Kristina Anderson-Teixeira, Heidi Asbjornsen, Luiza Maria T. Aparecido, Z. Carter Berry, Christopher Baraloto, Damien Bonal, Isaac Borrego, et al.

Charlotte Grossiord, Bradley Christoffersen, Aura Alonso-Rodríguez, Kristina Anderson-Teixeira, Heidi Asbjornsen, et al.. Precipitation mediates sap flux sensitivity to evaporative demand in the neotropics. Oecologia, 2019, 191 (3), pp.519-530. 10.1007/s00442-019-04513-x . hal-02346487

Grossiord, C., Christoffersen, B., Alonso-Rodríguez, A. M., Anderson-Teixeira, K., Asbjornsen, H., Aparecido, L. M. T., … McDowell, N. G. (2019). Precipitation mediates sap flux sensitivity to evaporative demand in the neotropics. Oecologia. https://doi.org/10.1007/s00442-019-04513-x

Precipitation mediates sap flux sensitivity to evaporative demand in the neotropics

Charlotte Grossiord[1,2]*, Bradley Christoffersen[3]*, Aura M. Alonso-Rodríguez [4], Kristina Anderson-Teixeira[5,6], Heidi Asbjornsen[7], Luiza Maria T. Aparecido[8,9], Z. Carter Berry[10], Christopher Baraloto[11], Damien Bonal[12], Isaac Borrego[2], Benoit Burban[13], Jeffrey Q. Chambers[14,15], Danielle S. Christianson[16], Matteo Detto[17,18] , Boris Faybishenko[14], Clarissa G. Fontes[19], Claire Fortunel[20,21], Bruno O. Gimenez[22], Kolby J. Jardine[15], Lara Kueppers[14], Gretchen R. Miller[23], Georgianne W. Moore[9], Robinson Negron-Juarez[14], Clément Stahl[13], Nathan G. Swenson[24], Volodymyr Trotsiuk[1,25,26], Charu Varadharajan[14], Jeffrey M. Warren[27], Brett T. Wolfe[18,28], Liang Wei[2], Tana E. Wood[4], Chonggang Xu[2], Nate G. McDowell[29]

* These two authors contributed equally to this work.

[1]Swiss Federal Institute for Forest, Snow and Landscape Research WSL, Zürcherstrasse 111, 8903 Birmensdorf, Switzerland

[2]Earth and Environmental Sciences Division, Los Alamos National Laboratory, Los Alamos, NM, USA

[3]Department of Biology and School of Earth, Environmental, and Marine Sciences, University of Texas Rio Grande Valley, Edinburg, TX, USA

[4]USDA Forest Service, International Institute of Tropical Forestry, Jardín Botánico Sur, 1201 Calle Ceiba, Río Piedras, PR 00926-1115, USA

[5]Center for Tropical Forest Science-Forest Global Earth Observatory, Smithsonian Tropical Research Institute, Panama City, Panama

[6]Conservation Ecology Center, Smithsonian Conservation Biology Institute, Front Royal, VA, USA

[7]Department of Natural Resources and the Environment, University of New Hampshire, Durham, NH 03824, USA

[8]School of Life Sciences, Arizona State University, AZ, USA

[9]Department of Ecosystem Science and Management, Texas A&M University, College Station, TX, USA

[10]Schmid College of Science and Technology, Chapman University, Orange, CA, USA

[11]International Center for Tropical Botany (ICTB), Department of Biological Sciences, Florida International University, Miami, FL, USA

[12]Université de Lorraine, AgroParisTech, INRA, UMR Silva, 54000 Nancy, France

[13]INRA, UMR EcoFoG, CNRS, Cirad, AgroParisTech, Université des Antilles, Université de Guyane, 97310 Kourou, France

[14]Department of Geography, University of California, Berkeley, Berkeley, CA, United States

[15]Climate and Ecosystem Sciences Division, Lawrence Berkeley National Laboratory, Berkeley, CA, United States

[16]Computational Research Division, Lawrence Berkeley National Laboratory, Berkeley, CA, USA

[17]Department of Ecology and Evolutionary Biology, Princeton University, Princeton, NJ, USA

[18]Center for Tropical Forest Science, Smithsonian Tropical Research Institute, Panamá, República de Panamá

[19]Department of Integrative Biology, University of California Berkeley, Berkeley, CA 94720-3140, USA

[20]Department of Integrative Biology, University of Texas at Austin, Austin, TX, USA

[21]AMAP (botAnique et Modélisation de l'Architecture des Plantes et des végétations), IRD, CIRAD, CNRS, INRA, Université de Montpellier, Montpellier, France

[22]Instituto Nacional de Pesquisas da Amazônia (INPA), Brazil

[23]Zachry Department of Civil Engineering, Texas A&M University, 3136 TAMU, College Station, TX, USA

[24]Department of Biology, University of Maryland, College Park, MD, USA

[25]ETH Zurich, Department of Environmental Systems Science, Institute of Agricultural Sciences, 8092 Zurich, Switzerland

[26]Czech University of Life Sciences Prague, Faculty of Forestry and Wood Sciences, Kamýcká 129, Praha 6, Suchdol 16521, Czech Republic

[27]Climate Change Science Inst. and Environmental Sciences Division, Oak Ridge National Laboratory, Oak Ridge, TN, USA

[28]School of Renewable Natural Resources, Louisiana State University, Baton Rouge, LA, USA

[29]Earth Systems Science Division, Pacific Northwest National Laboratory, Richland, WA, USA

Corresponding author: Charlotte Grossiord, charlotte.grossiord@wsl.ch, +41447392069

Author Contributions: CG, BC, JW and NGM planned the research. AA, HA, BB, BG, BW, CB, CB, CS, CF, DB, DC, MD, BF, CF, KJ, GRM, GWM, CV, JW, BW, NS, LA, TEW and LW contributed data. CG and BC analyzed the data and wrote a first draft of the manuscript, and all authors contributed to revisions.

Abstract

Transpiration in humid tropical forests modulates the global water cycle and is a key driver of climate regulation. Yet, our understanding of how tropical trees regulate sap flux in response to climate variability remain elusive. With a progressively warming climate, atmospheric evaporative demand (i.e., vapor pressure deficit, VPD) will be increasingly important for plant functioning, becoming the major control of plant water use in the 21st century. Using measurements in 34 tree species at seven sites across a precipitation gradient in the neotropics, we determined how the maximum sap flux velocity (v_{max}) and the VPD threshold at which v_{max} is reached (VPD_{max}) vary with precipitation regime (mean annual precipitation, MAP; seasonal drought intensity, P_{DRY}) and two functional traits related to foliar and wood economics spectra (leaf mass per area, LMA; wood specific gravity, WSG). We show that, even though v_{max} is highly variable within sites, it follows a negative trend in response to increasing MAP and P_{DRY} across sites. LMA and WSG exerted little effect on v_{max} and VPD_{max}, suggesting that these widely-used functional traits provide limited explanatory power of dynamic plant responses to environmental variation within hyper-diverse forests. This study demonstrates that long-term precipitation plays an important role in the sap flux response of humid tropical forests to VPD. Our findings suggest that under higher evaporative demand, trees growing in wetter environments in humid tropical regions may be subjected to reduced water exchange with the atmosphere relative to trees growing in drier climates.

Keywords: evapotranspiration, plant functional traits, transpiration, vapor pressure deficit.

Introduction

Humid tropical forests cover approximately 12% of global ice-free land surface area (Mayaux et al. 2005) and are characterized by high mean annual precipitation (> 1500 mm) with low variability in atmospheric temperature (≈ 25 ± 5°C) (Richards 1952; Murphy and Lugo, 1986). The majority of water entering tropical forests through precipitation or rivers is returned to the atmosphere via evapotranspiration (Moreira et al. 1997; Kumagai et al. 2016). Water released by trees in their transpiration flux largely contributes to total evapotranspiration in the tropics (Schlesinger and Jasechko 2014), 35% of which is cycled back to the biome as precipitation (Eltahir and Bras 1994; Zemp et al. 2014). As such, tree transpiration in tropical forests is a major modulator of the global water cycle and plays a central role in climate regulation (Foley et al, 2007). Yet, despite our efforts in understanding transpiration patterns of tropical trees (e.g., Meinzer et al. 2003; Stahl et al. 2013a; Maréchaux et al. 2018), how trees regulate water use in these ecosystems remains one of the largest uncertainty components in models of tropical evapotranspiration.

At daily to seasonal time-scales, trees regulate their transpiration flux in response to variation in atmospheric evaporative demand (i.e., vapor pressure deficit, *VPD*), radiation, wind and available soil water (Oren et al. 1999; Meinzer et al. 2001). Under non-limiting soil water availability, radiation and *VPD* are usually the most significant climate variables controlling water flux in tropical trees (e.g., Meinzer et al. 2008). However, global warming will result in an exponential climb in *VPD* in the next decades (Zhang et al. 2015), and the relative role of these two abiotic drivers (i.e., radiation *vs*. *VPD*) is expected to shift in the future with *VPD* becoming the major control of plant water use in the 21st century (Novick et al. 2016). Therefore, improving our understanding of water use patterns and their response to *VPD*, including the linkages to predictive plant traits, is an important next step with major implications for global climate and vegetation predictions.

While over long periods (i.e. years to decades), stand water use is mainly regulated by changes in leaf area and species composition, over short-term periods (i.e. hours to days), trees regulate sap flux velocity (v) (Edwards et al. 1996) through changes in stomatal conductance. Thus, v response to daily VPD variation directly depends on the degree of stomatal closure (Schulze et al. 1972). Under low VPD conditions, plant stomata are fully open and v increases linearly with VPD (Franks et al. 1997), until v reaches a saturation rate (v_{max}, Fig. 1) at a given VPD threshold (VPD_{max}, Fig. 1). As VPD increases, trees progressively start closing their stomata, and for some species, including tropical trees, stomatal closure can be so pronounced as to result in a decreased rate of v (Fig. 1) (Schulze et al. 1972; Franks et al. 1997). The degree of sap flux response to VPD varies both within and between species because of differences in local climatic adjustments and ecological strategy. For instance, trees originating from distinct precipitation regimes should differ in their sap flux responses to VPD because of adaptive mechanisms in response to moisture conditions, including wood hydraulic properties and foliar traits (Mencuccini 2003; Poyatos et al. 2007). Trees growing in drier climates may produce xylem elements with reduced lumen areas relative to trees from wetter climates to reduce the risk of xylem embolism and promote overall hydraulic safety (Hacke et al. 2004; Fonti and Jansen 2012). Anatomical changes in these conductive tissues will directly alter the sap flux patterns of trees (i.e. reduced v in drier systems), and have been associated to reduced VPD_{max} and v_{max} in dry ecosystems (Grossiord et al. 2017; 2018). Similarly, reductions in soil moisture during dry periods have been linked with changes in stomatal density (Luomala et al. 2005) and in the synthesis of chemical signals inducing stomatal closure (Schachtman and Goodger 2008), which should also reduce VPD_{max} and v_{max} in forests that are subjected to seasonal droughts. In humid tropical forests, regional variability in annual precipitation (from 1500 to > 4000 mm annually) and in dry season intensity is high, suggesting large variation in plant physiological and structural adjustments to moisture status, and thus potentially important differences in VPD_{max} and v_{max} between ecosystems. However, soil moisture is usually less limiting in humid tropical forests than in temperate and semiarid regions where reductions in VPD_{max} and v_{max} following precipitation reduction have been reported (Grossiord et al. 2018). As such, this characteristic physiological or hydraulic adjustment to soil moisture limitation may not occur in this biome, suggesting that acclimation processes to water stress would only occur under a given precipitation and/or drought intensity threshold.

A difficulty in making predictions on the functioning of humid tropical forests lies in the fact that these ecosystems host more tree species than any other terrestrial ecosystem (Myers et al. 2000). Large species diversity in the tropics is accompanied by large diversity in plant functional traits (Wright et al. 2007; Baraloto et al. 2010; Fortunel et al. 2012; 2014; Zhu et al. 2013; Cosme et al. 2017). Functional differences that directly alter v regulation include rooting properties (e.g. water uptake depth, Stahl et al. 2013b; Brum et al. 2019), hydraulic properties (e.g. lumen area or water potential at 50% loss of hydraulic conductivity P_{50}; Litvak et al. 2012) and foliar characteristics (e.g. stomatal density or leaf turgor loss point; Bartlett et al. 2012, Maréchaux et al. 2018). However, while such mechanistic trait data are growing in availability for tropical forests, they remain poorly quantified relative to more easily measurable traits such as leaf mass per area (*LMA*) and wood specific gravity (*WSG*) (Wright et al. 2004; Chave et al. 2014). *LMA* and *WSG* respectively comprise the well-studied leaf and wood economics spectra, which have been successfully related to various aspects of plant function along a fast (resourceacquisitive, low *LMA* and *WSG*)-to-slow (resource-conservative, high *LMA* and *WSG*) continuum (Reich et al. 1997; but see Baraloto et al. 2010; Fortunel et al. 2012). These traits only indirectly relate to dynamic physiological processes such as F_D (Brodribb 2017), however *LMA* and *WSG* can be used to support mechanistic theory of moisture adjustments in modelling frameworks by correlating with other plant traits related to hydraulic transport (Christoffersen et al. 2016). As such, we might expect trees originating from drier regions in humid tropical forests, and thus with lower VPD_{max} and v_{max}, to have higher *LMA* and *WSG* (i.e. two typical adjustment responses to reduced moisture, Wright et al. 2005) relative to trees with higher VPD_{max} and v_{max}.

Here we analyzed how trees regulate sap flux velocity in response to *VPD* variation in 34 species originating from seven sites along a precipitation gradient in the neotropics. Our objectives were to test how long-term local precipitation regime (annual precipitation and intensity of the dry season) modulate VPD_{max} and v_{max}, and detect whether variation in VPD_{max} and v_{max} across sites can be related to the variability in two easy-to-measure functional traits: *LMA* and *WSG*. We hypothesized that:

1) trees growing in relatively dry regions and that are subjected to more frequent and intense droughts would show reduced VPD_{max} and v_{max} compared to trees originating from wetter areas because of long-term physiological and structural adjustments to reduced soil moisture availability (Mencuccini 2003) (Fig. 1),
2) across all sites, trees with higher *LMA* and *WSG* would show reduced VPD_{max} and v_{max} relative to trees with low *LMA* and *WSG*.

Material and methods

Study sites

We used data collected from mature humid tropical forests in seven sites spanning from Puerto Rico to northern Brazil (Table 1, Figs. S1 & S2). The focal sites are located in Puerto Rico (SAB hereafter), Costa Rica (SOL), Panama (SLZ, BCI and PNM), French Guiana (FRG) and Brazil (MAN). The target tree species pool (representing among the most abundant tree species within each site) varied between four and nine per site (Table 2), leading to a total of 34 tree species included in this study with only one species being present at multiple sites (Table S1). Climatic conditions (rainfall, air temperature, atmospheric humidity and solar radiation) were measured continuously and recorded by local weather stations at all sites during the measurements.

All sites, apart from the SOL site, experience a dry season (i.e., monthly precipitation < 100 mm) of approx. three months. Long-term precipitation was used to characterize long-term annual moisture status and drought intensity in each site using the site-level average in annual sum of precipitation (MAP) and monthly precipitation during the dry season (P_{DRY}) over the 1950-2010 period. When long-term site-specific data was not available (all sites except PNM, BCI and SLZ), long-term precipitation was extracted for each site using Twentieth Century Reanalysis Project, a 2.0-degree latitude and 2.0-degree longitude global climate dataset (Compo et al. 2011). The sites were characterized by contrasting precipitation regimes varying between 1826 and 4200 mm on average annually over the 1950-2010 period, with the PNM site (Panama) being the driest and the SOL site (Costa Rica) the wettest (PNM < MAN < BCI < SLZ < FRG < SAB < SOL) (Table 1). See Table 1 for more details on site characteristics and site-specific references.

Sap flux measurements

In each site between four and nine trees that occupied dominant positions in the canopy (to avoid effects related to crown exposure) were selected for this study, leading to a total of 43 trees (Table 2). At all sites, tree sap flux velocity (v; cm h^{-1}) was measured every 10 min, 15 min, 30 min or hour using either the thermal dissipation method (Granier 1987) or the heat ratio method (Burgess et al. 1998). Depending on the site, sensors were bought from manufacturers (SFM1, ICT International, NSW, Australia; UP-Gmbh, Cottbus, Germany; PS-GP, PlantSensors, Nakara, Australia) or lab-built. Measurements were conducted continuously for periods varying between two and 24 months (Table 1) between January 2014 and January 2017. For the thermal dissipation method, sensors (i.e. one sensor per tree except for the SOL site where two sensors per tree were installed, 10- or 20-mm long) were installed in the sapwood at 1.3 m aboveground or above buttresses with a 10 cm vertical spacing between probes. For the heat-ratio method (i.e. one sensor per tree), each set of sensors consisted of two or three thermocouples and one-line heater probe. The thermocouples were inserted at 1.3 m aboveground at depths varying between 2.2 and 3 cm below the cambium. The sensors were covered with reflective insulation to reduce the risk of direct sunlight causing thermal gradients. The data were recorded continuously by dataloggers (CR800, CR10X and CR1000, Campbell Scientific Corp., Logan, UT, USA), apart from the SFM1 sensors that contain a stand-alone datalogger. For more details see the site-specific references in Table 1.

Sap flux data processing

Each site's sap flux data files were accompanied by a standardized metadata reporting framework, consisting of three associated metadata files, respectively describing the data files, the columns of each data file, and field observations of tree size, canopy position, and species identity, if available (Christianson et al. 2017). We collated the raw data for all sites via a series of R scripts, which interpreted each dataset in terms of its associated metadata file (code available in the supplement of Christianson et al. 2017).

We started data processing using the raw mV values outputted by the sap flux sensors. Sap flux velocity data from the SOL site had already been converted to v (cm h^{-1}) using the Granier equation (1987) (see Aparecido et al. 2016 for more details). The open-source *Baseliner* software (Oishi et al. 2016) was used to calculate v values for each tree following the equation proposed by Granier (1987). No species-specific equations are available for the tropical species included in this study, and thus care must be taken when interpreting v results as the empirically derived coefficients in the Granier equation may introduce errors in v calculations (Bush et al. 2010). *Baseliner* enables users to control the quality and process data using a combination of automated steps and manual editing (Oishi et al. 2016). Missing data were gap filled when they were shorter than two hours using linear interpolation (Oishi et al. 2016). Estimation of baseline nighttime flow is done automatically in *Baseliner* based on a joint set of conditions, including nighttime hours (characterized by near-zero radiation), stable temperature differential between probes (estimated using coefficient of variation) and low *VPD* (see Oishi et al. 2016 for more details).

After converting all values into v, we conducted a systematic removal of values associated with measurement failures and sensor removals in the field. For the MAN, PNM, SLZ and BCI sites, we removed all days before DOY 175 in 2016 (corresponding to the 2015-2016

ENSO event) to avoid potential *v* responses to anomalously low soil moisture (Fig. S3). In addition, sub-hourly *v* data was visually assessed for all trees to ensure no drought period was included in the final dataset. The FRG site included semi-deciduous tree species, which experienced leaf drop during the measurement periods. To avoid effects related to changes in leaf area induced by significant leaf drop, these periods were removed from the analyses. Individual-tree *v* time series are presented for each site in Fig. S4. The two methods used for measuring *v* (heat ratio method *vs*. thermal dissipation method) have been shown to vary in their accuracy to measure absolute *v* rates (Steppe et al. 2010). However, tests conducted at the MAN and SLZ sites (i.e. the two sites where the heat ratio method was used), where both sensor types were collocated on individual trees, indicated no significant differences in *v* rates between the two methods (Fig. S5). No information on the depth of the active sapwood was available for the target trees, but to our knowledge, no study reported radial changes in *v* patterns to *VPD* variation.

Estimation of maximum sap flux velocity and VPD at which sap flux velocity reaches maximum values

To avoid confounding effects of radiation we applied a radiation filter for each site by removing all *v* data where sub-hourly radiation was below the 90th percentile of daytime radiation values. For most sites this threshold was equal to 600 W m^{-2} apart for the BCI and FRG sites where the threshold was equal to 700 W m^{-2} (Fig S6). Using sub-hourly *v* data, we estimated the maximum sap flux velocity (v_{max}, Fig. 1) for each tree as the 95th percentile of *v* values after applying the radiation filter (Fig. S7). The *VPD* value at which *v* reaches maximum levels (VPD_{max}, Fig. 1) was estimated as the 2.5th percentile of *VPD* values corresponding to v_{max} (Fig.

S7). All the analysis was done using the R language for statistical computing (3.2.1, R Development Core Team 2015).

Functional traits

To analyze how variation in VPD_{max} and v_{max} could be related to foliar and wood functional traits, we used leaf mass per area (*LMA*, g m^{-2}) and wood specific gravity (*WSG*, g cm^{-3}). Investigation of other traits (e.g., wood anatomy, leaf-to-sapwood area ratio) revealed a paucity of data for the target tree species, thus we focused strictly on *LMA* and *WSG*. When possible, we used direct measurements on the sampled trees during the sap flux measurements. Conversely, when the trait measurements were not available for our focal trees, we used previously published data originating from the same species (see sources in Table S1). In total, data on *LMA* and *WSG* were gathered for 31 (73%) and 39 (91%) trees (for *LMA* and *WSG*, respectively) (Table S1).

Statistical analyses

The impacts of long-term *MAP* (or P_{DRY}), *LMA* and *WSG* on VPD_{max} and v_{max} were determined first by fitting linear models, followed by closer examination using linear mixed effect models (package *lme*) where *MAP* (or P_{DRY}), *LMA*, *WSG*, diameter at breast height (*DBH*, i.e. to account for effects related to tree size) and their interactions were used as fixed effects, and trees nested in sites was used as a random effect. The model selection procedure started with all variables and by progressively removing the variables with the lowest explanatory power until the minimal model with the lowest Akaike Information Criterion (AIC) was obtained.

Models were compared using ‘anova’ test to select the least complex parsimonious model. In all cases, the linear model (package *lm*) with *MAP* or P_{DRY} was selected. The same tests were used to detect the impact of *MAP* (or P_{DRY}) on *LMA* and *WSG*, with *MAP* (or P_{DRY}), *DBH* and their interaction used as fixed effects.

Results

Climatic conditions

Precipitation during the measurements was similar to the long-term average precipitation (1950-2010) in all sites (Fig. S3). Mean daily air temperature and *VPD* ranged from 18 to 28°C, and 0.47 to 2.94 kPa, respectively, during the measurement period, depending on the sites and seasons (Fig. S8). The sites experienced a range of *VPD* values during sap flux measurements varying between 0 and approx. 4.3 kPa (Fig. 2).

Sap flux response to VPD variation

Strong variability in sap flux velocity (*v*) was observed within sites, reflecting the important diversity of water use strategies between species (Fig. S4). For most trees, *v* increased linearly with *VPD* until reaching a saturation rate (v_{max}) at a given *VPD* threshold (VPD_{max}, Fig. 2). For a few trees, *v* decreased with rising *VPD* after reaching a saturation rate, suggesting strong stomatal closure, while other trees showed no distinctive saturation rate with rising *VPD* (Fig. 2). Trees displaying a decline in *v* at high *VPD* did not have significantly different *LMA* or *WSG* from trees without such a decline (Welch's two-sided t-test: t = 0.257, df = 4.05, *P* = 0.810; t = 0.169, df = 4.75, *P* = 0.873, respectively). In general, v_{max} was reached when VPD_{max} varied between 0.6 and 2.0 kPa, depending on the trees (Fig. 2). v_{max} varied between 4.1 and 41.4 cm h^{-1}, depending on the individual tree (Fig. 2).

VPD_{max} and v_{max} were highly variable across sites, with a tendency for lower mean values at wetter sites and higher values at drier sites. The driest site, PNM, had the highest values (mean of 1.5 kPa and 24.7 cm h^{-1} for VPD_{max} and v_{max}, respectively), while the wettest site, SOL, had the lowest v_{max} (mean of 7.7 cm h^{-1}). There were significant negative effects of *MAP* on v_{max} ($r^2 = 0.32$, slope = -0.006, $P < 0.001$) but not on VPD_{max} ($r^2 = 0.10$, slope = -0.000, $P = 0.062$) (Fig. 3). A significant negative effect of P_{DRY} was found for v_{max} ($r^2 = 0.21$, slope = -0.21, $P = 0.005$), but not for VPD_{max} ($r^2 = 0.00$, slope = -0.000, $P = 0.842$) (Fig. 3). No relationship was found between VPD_{max} and v_{max} (Fig. S9), indicating no trade-off between the *VPD* threshold at which *v* levels-off at maximum rates and maximum *v*.

Relationships with functional traits

No effect of *LMA* on v_{max} ($r^2 = 0.00$, $P = 0.835$), and VPD_{max} ($r^2 = 0.00$, $P = 0.704$) was found. Similarly, no relationship between *WSG* and v_{max} ($r^2 = 0.08$, $P = 0.167$), and VPD_{max} ($r^2 = 0.02$, $P = 0.542$) were found (Fig. 4). There was no effect of *MAP* or P_{DRY} on *LMA* ($P = 0.722$ and $P = 0.600$, respectively), nor on *WSG* ($P = 0.434$ and $P = 0.290$). A significant relationship was observed between *LMA* and *WSG* (Fig. S9), suggesting a slight coupling between leaf and stem economics in these trees (i.e. trees with higher *LMA* tend to grow denser wood).

Discussion

Precipitation mediates sap flux response to evaporative demand in the neotropics

Our findings highlight that sap flux response to *VPD* under non-depleted soil moisture conditions in humid tropical forests partially depends on average *MAP* and P_{DRY} over the last 50 years, i.e., indicators of long-term moisture availability and drought stress intensity. More specifically, our data show that as average site-level precipitation increases and seasonal drought intensity decreases, trees attain lower maximum sap flux (v_{max}) when soil moisture is non-limiting (Fig. 3). This relationship was not an artefact of reduced radiation at wetter sites because of the radiation filter applied (Fig. S6). These findings contrast with previous observations from Mediterranean and semiarid woodlands where increasing aridity resulted in reduced v_{max} (e.g., Poyatos et al. 2007; Grossiord et al. 2018), suggesting contrasting underlying adjustments to moisture between supply-limited and demand-limited environments.

The negative response pattern of v_{max} to increasing *MAP* and P_{DRY} observed here implies that compared to dry temperate forests, tree sap flux velocity in humid tropical forests does not depend on drought-adjustments to local climate (i.e. adjustments reducing the vulnerability to water shortage) (Grossiord et al. 2018). Instead, sap flux patterns in response to climate variability are probably dependent on adjustments to high-moisture conditions. Indeed, in the sites included here, *VPD* is usually low and precipitation is high compared to temperate and semiarid regions, thus tree water relations are more rarely limited by high evaporative demand or drought stress. One may therefore expect trees in this environment to have evolved functional traits to deal with other limiting factors such as low radiation induced by the high cloud cover (Moore et al. 2018). Furthermore, high atmospheric humidity can lead to sustained leaf wetness with water films on leaves inhibiting gas exchanges, and resulting in reduced sensitivity to atmospheric drivers (Dawson and Goldsmith 2018; Moore et al. 2018). Plants that grow in high atmospheric humidity conditions have also been reported to show low levels of endogenous abscisic acid (ABA) (Nejad and Van Meeteren 2007; Okamoto et al. 2009), and marginal stomata regulation on carbon and water fluxes (Torre and Fjeld 2001; Torre et al. 2003). Therefore, an important research topic for future work, in addition to exploring adjustment mechanisms to reduced precipitation, is to understand how adaptive mechanisms related to high moisture could relate to sap flux regulation in tropical trees.

Lower v_{max} under non-limiting soil moisture conditions could potentially result in reduced water exchange with the atmosphere in humid tropical forests as more days with high *VPD* are likely to occur in the future. Currently, Earth system models (ESM) are being developed to incorporate plant hydraulic traits (Xu et al. 2016, Christoffersen et al. 2016, Kennedy et al. 2019), but it is not immediately clear if such traits will produce the patterns observed here for humid tropical ecosystems. Incorporating traits related to adjustments to high-moisture environments could potentially affect the differential responses of global precipitation to vegetation changes (e.g., Kooperman et al. 2018). To gain further insight into the drivers of sap flux variability, we suggest extending this work to more extreme sites, i.e. both wet and dry, and exploring other relevant factors such as long-term indices of evaporative demand (Poyatos et al. 2007). Improved quantification of within-site variation, including systematic replication of species sampled along environmental gradients would also be needed. Such an improved design would be valuable for trait-enabled dynamic vegetation models (Fisher et al. 2018), even if systematically sampling the same species in tropical forests may prove complicated considering their high species diversity.

Common functional traits provide limited insights into the mechanisms of sap flux regulation in the neotropics

We found a large variability in *LMA* and *WSG* within and across sites, reflecting the high functional diversity present in these ecosystems (Fortunel et al. 2012). Nevertheless, the large diversity in these functional traits could not be related to the variability in VPD_{max} and v_{max} observed across sites (Fig. 4). This is not so surprising in light of a recent review (Moles 2018) that highlights a remarkable degree of inconsistency in reported relationships of *LMA* and *WSG* with other plant traits related to plant ecological strategy or the fast-slow economic spectrum (Reich 2014). Moreover, we expect that stem and leaf traits more directly related to acquisition, transport, and retention of water (hydraulic traits) would underpin the patterns observed here; appropriate trait selection is therefore critical for uncovering trait-moisture relationships more generally (Griffin-Nolan et al. 2018). Specifically, reduction in moisture across large environmental gradients has been associated with shifts in mechanistic foliar traits such as stomatal density (e.g. Luomala et al. 2005) or chemical compounds inducing stomatal closure (Schachtman and Goodger 2008). Investigating such anatomical and chemical foliar adjustments that provide stronger mechanistic basis than *LMA* will be needed to unravel the underlying adaptive processes driving VPD_{max} and v_{max} patterns along our precipitation gradient (Fig. 3). Similarly, *WSG* had no detectable impact on VPD_{max} and v_{max} (Fig. 4). Wood density is considered an important modulator of xylem water transport as higher wood density has been associated with reduced hydraulic conductivity and higher resistance to xylem cavitation (Hacke et al. 2004). As such, this property could constrain the maximum flux of water movement in trees (Barbour and Whitehead 2003). However, most *WSG* measurements, including the ones used in this study, are made using main stems. Yet, to be relevant for water transport, this trait should represent all woody tissues, from the roots to the canopy (Fortunel et al. 2012). Furthermore, the interpretation of *WSG* as an indicator of plant hydraulic functions is debated (Larjavaara and Muller-Landau 2010), since a given *WSG* can be achieved under various combinations of wood anatomy which do not necessarily impact water transport, but instead reflect variability in the competing demands of strength and storage (Fortunel et al. 2014; Zieminska et al. 2015; Morris et al. 2016; Dias et al. 2019).

Therefore, although *LMA* and *WSG* are useful for indicating, respectively, placement on the leaf economics spectrum (Wright et al. 2004) and successional status in productivity models (Moorcroft et al. 2001), they do so only at global scales and do not consistently relate to other plant traits at local and regional scales (Moles 2018), as our findings also confirm here. They appear to provide limited interpretation of dynamic plant responses to environmental variation within hyper-diverse tropical forests (Brodribb 2017). While incorporation of such local adjustments in ESMs is possible via trait-mediated plant responses to the environment (e.g., Fisher et al. 2015), the functional traits explored here, *LMA* and *WSG*, show little promise. Focused data collection on more mechanistic traits associated with plant hydraulics and stomatal function like for instance P_{50}, leaf turgor loss point, cuticular conductance, sapwood anatomy, stomatal density or foliar chemical compounds are likely to reveal mechanistic controls on the interspecific differences in sap flow observed here, which can be used to refine existing plant hydraulic models (Christoffersen et al. 2016; Wolf et al. 2016; Xu et al. 2016; Sperry et al. 2017).

Conclusion

This study demonstrates that local climate plays an important role in the sap flux response of humid tropical forests to evaporative demand. Moreover, we highlight that trees growing in wetter regions in the tropics may be subjected to a reduced sap flux velocity with the high evaporative demand predicted by most climate models. We expect incorporating these regulation strategies in models could improve our prediction accuracy of both vegetation dynamics and water cycles. This study also shows that easy-to-measure functional traits provide little interpretation in dynamic sap flux response to *VPD*, suggesting that more mechanistic traits should be investigated to build predictors in future models. Finally, it is important to note that although our sampling included a large number of species relative to previous studies investigating sap flux-climate responses, our work still covers only a limited range of the incredible diversity present in humid tropical forests. Extending sap flux measurements in more regions in the tropics and developing large databases of plant water use (e.g. SAPFLUXNET, Poyatos et al. 2016) is an important next step if we want to improve our predictive capacity of tropical forest responses to climate change.

Acknowledgments

This project was supported in part by the Next Generation Ecosystem Experiments Tropics, funded by the US Department of Energy, Office of Science, Office of Biological and Environmental Research, Terrestrial Ecosystem Sciences Program, under Award Number DE-SC-0011806. CG was supported by the Swiss National Science Foundation SNF (5231.00639.001.01). BC was supported in part by the Laboratory Directed Research and Development Program Project 8872 of Oak Ridge National Laboratory, managed by UT-Battelle, LLC, for the U. S. Department of Energy. This work has benefited from an “Investissements d’Avenir” grant managed by Agence Nationale de la Recherche (CEBA, ref. ANR-10-LABX-25-01). Data recorded in French Guiana (FRG) were collected at the Guyaflux sites which belong to the SOERE F-ORE-T and is supported annually by Ecofor, Allenvi and the French national research infrastructure, ANAEE-F. We thank Valentine Herrmann for building the probes for the Panamanian and Brazilian sites. We thank all technicians, students and post-docs who helped collect data at all sites.

References

Aparecido LMT, Miller GR, Cahill AT, Moore GW (2016) Comparison of tree transpiration under wet and dry canopy conditions in a Costa Rican premontane tropical forest. Hydrological Processes 30, 26: 5000-5011.

Baraloto C, Timothy Paine CE, Poorter L, Beauchene J, Bonal D, Domenach A-M, Hérault B, Patiño S, Roggy J-C, Chave J (2010) Decoupled leaf and stem economics in rain forest trees. Ecology Letters 13: 1338-1347.

Barbour MM, Whitehead D (2003) A demonstration of the theoretical prediction that sap velocity is related to wood density in the conifer Dacrydium cupressinum. New Phytologist 158: 477–488.

Bartlett MK, Scoffoni C, Sack L (2012) The determinants of leaf turgor loss point and prediction of drought tolerance of species and biomes: a global meta‐analysis. Ecology Letters 15: 393-405.

Bonal D, Bosc A, Ponton S, Goret J-Y, Burban B, Gross P, Bonnefond J-M, Elbers J, Longdoz B, Epron D, Guehl J-M, Granier A (2008) Impact of severe dry season on net ecosystem exchange in the Neotropical rainforest of French Guiana. Global Change Biology 14: 1917-1933.

Brodribb TJ (2017) Progressing from ‘functional’ to mechanistic traits. New Phytologist 215: 9-11.

Brum M, Vadeboncoeur MA, Ivanov V, Asbjornsen H, Saleska S, Alves LF, Penha D, Dias JD, Aragão LE, Barros F, Bittencourt P (2019) Hydrological niche segregation defines forest structure and drought tolerance strategies in a seasonal Amazon forest. Journal of Ecology, https://doi.org/10.1111/1365-2745.13022

Burgess SS, Adams MA, Turner NC, Ong CK (1998) The redistribution of soil water by tree root systems. Oecologia 115: 306-311.

Burgess SS, Adams MA, Turner NC, Beverly CR, Ong CK, Khan AA, Bleby TM (2001) An improved heat pulse method to measure low and reverse rates of sap flow in woody plants. Tree Physiology 21: 589-598.

Bush SE, Hultine KR, Sperry JS, Ehleringer JR (2010) Calibration of thermal dissipation sap flow probes for ring-and diffuse-porous trees. Tree Physiology 30: 1545-1554.

Cate RB, Nelson LA (1971) A simple statistical procedure for partitioning soil test correlation data into two classes. Soil Science Society of America Proceedings 35: 658-660.

Chave J, Rejou-Mechain M, Burquez A, Chidumay E, Colgan MS, Delitti WBC et al. (2014) Improved allometric models to estimate the aboveground biomass of tropical trees. Global Change Biology 20: 3177–3190.

Christianson DS, Varadharajan C, Christofferson B, Detto M, Faybishenko BA, Jardine KJ, Negron-Juarez R, Gimenez BO, Pastorello GZ, Powell T, Warren J, Wolfe B, Chambers JC, Kueppers LM, McDowell NG, Agarwal D (2017) A metadata reporting framework for standardization and synthesis of ecohydrological field observations for ecosystem model parameterization and benchmarking. Ecological Informatics 42: 148-58.

Christoffersen BO et al. (2016) Linking hydraulic traits to tropical forest function in a size-structured and trait-driven model (TFS v. 1-Hydro). Geoscientific Model Development 9: 4227.

Compo GP et al. (2011) The Twentieth Century Reanalysis Project. Quarterly Journal of the Royal Meteorological Society 137: 1-28.

Cosme LHM, Schietti J, Costa FRC, Oliveira RS (2017) The importance of hydraulic architecture to the distribution patterns of trees in a central Amazonian forest. New Phytologist 215: 113-125.

Dawson TE, Goldsmith GR (2018) The value of wet leaves. New Phytologist 219: 1156-1169.

Detto M, Wright SJ, Calderón O, Muller-Landau HC (2018). Resource acquisition and reproductive strategies of tropical forest in response to the El Niño–Southern Oscillation. Nature communications 9: 913.

Dias AS, Oliveira RS, Martins FR, Bongers F, Anten NPR, Sterck F (2019) How do lianas and trees change their vascular strategy in seasonal versus rain forest? Perspectives in Plant Ecology, Evolution and Systematics 40: 125465.

Edwards WRN, Becker P, Èermák J (1997). A unified nomenclature for sap flow measurements. Tree Physiology 17: 65-67.

Eltahir EAB, Bras RL (1994). Precipitation recycling in the Amazon basin. Quarterly Journal of the Royal Meteorological Society 120: 861-880.

Fauset S, Baker TR, Lewis SL, Feldpausch TR, Affum-Baffoe K, Foli EG, Hamer KC, Swaine MD, Etienne R (2012) Drought-induced shifts in the floristic and functional composition of tropical forests in Ghana. Ecology Letters 15: 1120-1129.

Fisher RA et al. (2015) Taking off the training wheels: the properties of a dynamic vegetation model without climate envelopes, CLM4. 5 (ED). Geoscientific Model Development 3593-3619.

Fisher RA et al. (2018) Vegetation demographics in Earth System Models: A review of progress and priorities. Global Change Biology 24: 35-54.

Foley JA et al. (2007) Amazonia revealed: forest degradation and loss of ecosystem goods and services in the Amazon Basin. Frontiers in Ecology and the Environment 5: 25-32.

Fonti P, Jansen S (2012) Xylem plasticity in response to climate. New Phytologist 195: 734-736.

Fortunel C, Fine PVA, Baraloto C, Dalling J (2012) Leaf, stem and root tissue strategies across 758 Neotropical tree species. Functional Ecology 26: 1153-1161.

Fortunel C, Ruelle J, Beauchene J, Fine PV, Baraloto C (2014) Wood specific gravity and anatomy of branches and roots in 113 Amazonian rainforest tree species across environmental gradients. New Phytologist 202: 79-94.

Franks PJ, Cowan IR, Farquhar GD (1997) The apparent feedforward response of stomata to air vapour pressure deficit: information revealed by different experimental procedures with two rainforest trees. Plant, Cell & Environment 20: 142-145.

Good SP, Moore GW, Miralles DG (2017) A mesic maximum in biological water use demarcates biome sensitivity to aridity shifts. Nature Ecology & Evolution 1: 1883.

Gleason SM, Butler DW, Zieminska K, Waryszak P, Westoby M (2012) Stem xylem conductivity is key to plant water balance across Australian angiosperm species. Functional Ecology 26: 343–352.

Granier A (1987) Evaluation of transpiration in a Douglas-fir stand by means of sap flow measurements. Tree Physiology 3: 309-320.

Griffin-Nolan RJ, Bushey JA, Carroll CJW, Challis A, Chieppa J, Garbowski M, Hoffmann AM, Post AK, Slette IJ, Spitzer D, Zambonini D (2018) Trait selection and community weighting are key to understanding ecosystem responses to changing precipitation regimes. Functional Ecology 32: 1746-1756.

Grossiord C, Sevanto S, Borrego I, Chan AM, Collins AD, Dickman LT, Hudson P, McBranch N, Michaletz ST, Pockman WT, Vilagrosa A, McDowell NG (2017) Tree water dynamics in a drying and warming world. Plant, cell & environment 40: 1861-1873

Grossiord C, Sevanto S, Limousin JM, Meir P, Mencuccini M, Pangle RE, Pockman WT, Salmon Y, Zweifel R, McDowell NG (2018) Manipulative experiments demonstrate how long-term soil moisture changes alter controls of plant water use. Environmental and Experimental Botany 152: 19-27

Hacke UG, Sperry JS, Pittermann J (2004) Analysis of circular bordered pit function II. Gymnosperm tracheids with torus-margo pit membranes. American Journal of Botany 91: 386-400.

Hogg EH, Hurdle PA (1997) Sap flow in trembling aspen: implications for stomatal responses to vapor pressure deficit. Tree Physiology 17: 501-509.

Kennedy D, Swenson S, Oleson KW, Lawrence DM, Fisher R, Lola da Costa AC, Gentine P (2019) Implementing plant hydraulics in the Community Land Model, version 5. Journal of Advances in Modeling Earth Systems 11: 485-513.

Kimball BA, Alonso-Rodríguez AM, Cavaleri MA, Reed SC, González G, Wood TE. (2018) Infrared heater system for warming tropical forest understory plants and soils. Ecology & Evolution, 8, 1932–1944.

Kooperman GJ et al. (2018) Forest response to rising CO_2 drives zonally asymmetric rainfall change over tropical land. Nature Climate Change 8 : 434.

Koenker R (2017) Quantreg: quantile regression. R package version 5.33. R Foundation for Statistical Computing, Vienna.

Kumagai T, Kanamori H, Chappell NA (2016) Tropical forest hydrology. Forest Hydrology: Processes, Management and Assessment 88-102.

Lange OL, Lösch R, Schulze ED, Kappen L (1971) Responses of stomata to changes in humidity. Planta 100: 76-86.

Larjavaara M, Muller-Landau HC (2010) Rethinking the value of high wood density. Functional Ecology 24: 701-705.

Limousin JM et al. (2012) Morphological and phenological shoot plasticity in a Mediterranean evergreen oak facing long-term increased drought. Oecologia 169: 565-577.

Litvak E, McCarthy HR, Pataki DE (2012) Transpiration sensitivity of urban trees in a semi-arid climate is constrained by xylem vulnerability to cavitation. Tree physiology 32: 373-388.

Luomala E, Laitinen K, Sutinen S, Kellomäki S, Vapaavuori E (2005) Stomatal density, anatomy and nutrient concentrations of Scots pine needles are affected by elevated CO2 and temperature. Plant, Cell & Environment 28: 733-749.

Luizão RC, Luizão FJ, Paiva RQ, Monteiro TF, Sousa LS, Kruijt B (2004) Variation of carbon and nitrogen cycling processes along a topographic gradient in a central Amazonian forest. Global Change Biology 10: 592-600.

Malhi Y, Wright J (2004) Spatial patterns and recent trends in the climate of tropical rainforest regions. Philosophical Transactions of the Royal Society B: Biological Sciences 359: 311-329.

Malhi Y (2009) Exploring the likelihood and mechanism of a climate-change-induced dieback of the Amazon rainforest. Proceedings of the National Academy of Sciences 106: 20610.

Mangiafico S (2018) rcompanion: Functions to Support Extension Education Program Evaluation. R package version 2.0.0. https://CRAN.R-project.org/package=rcompanion

Maréchaux I, Bonal D, Bartlett MK, Burban B, Coste S, Courtois EA, Dulormne M, Goret J-Y, Mira E, Mirabel A, Sack L, Stahl C, Chave J (2018) Dry-season decline in tree sapflux is correlated with leaf turgor loss point in a tropical rainforest. Functional Ecology, doi: 10.1111/1365-2435.13188.

Martinez-Cabrera HI, Jones CS, Espino S, Schenk HJ (2009) Wood anatomy and wood density in shrubs: responses to varying aridity along transcontinental transects. American Journal of Botany 96: 1388–1398.

Mayaux P, Holmgren P, Achard F, Eva H, Stibig HJ, Branthomme A (2005) Tropical forest cover change in the 1990s and options for future monitoring. Philosophical Transactions of the Royal Society B: Biological Sciences 360: 373-384.

Meinzer FC, Goldstein G, Andrade JL (2001) Regulation of water flux through tropical forest canopy trees: do universal rules apply? Tree Physiology 21: 19-26.

Meinzer FC, James SA, Goldstein G, Woodruff D (2003) Whole-tree water transport scales with sapwood capacitance in tropical forest canopy trees. Plant, Cell & Environment 26: 1147–1155.

Meinzer FC, Woodruff DR, Dome, J-C, Goldstein G, Campanello PI, Gatti MG, Villalobos-Vega R (2008) Coordination of leaf and stem water transport properties in tropical forest trees. Oecologia 156: 31–41.

Mencuccini M (2003) The ecological significance of long- distance water transport: short- term regulation, long- term acclimation and the hydraulic costs of stature across plant life forms. Plant, Cell & Environment 26: 163-182.

Moles AT (2018) Being John Harper: Using evolutionary ideas to improve understanding of global patterns in plant traits. Journal of Ecology 106:1-18.

Monteith JL (1995) A reinterpretation of stomatal responses to humidity. Plant, Cell & Environment 18: 357-364.

Moorcroft PR, Hurtt GC, Pacala SW (2001) A method for scaling vegetation dynamics: the ecosystem demography model (ED). Ecological monographs 71: 557-586.

Moore GW, Orozco G, Aparecido LM, Miller GR (2018) Upscaling transpiration in diverse forests: Insights from a tropical premontane site. Ecohydrology 11: e1920.

Moreira M *et* al. (1997) Contribution of transpiration to forest ambient vapor based on isotopic measurements. Global Change Biology 3: 439-450.

Morris H, Plavcová L, Cvecko P, Fichtler E, Gillingham MA, Martínez-Cabrera HI, McGlinn HI, Wheeler DJ, Zheng E, Ziemińska K, Jansen S (2016) A global analysis of parenchyma tissue fractions in secondary xylem of seed plants. New Phytologist 209: 1553-1565.

Murphy PG, Lugo AE (1986) Ecology of tropical dry forest. Annual review of ecology and systematics 17: 67-88.

Myers N, Mittermeier RA, Mittermeier CG, Da Fonseca GA, Kent J (2000) Biodiversity hotspots for conservation priorities. Nature 403: 853.

Nejad AR, Van Meeteren U (2007) The role of abscisic acid in disturbed stomatal response characteristics of Tradescantia virginiana during growth at high relative air humidity. Journal of Experimental Botany 58: 627–636.

Novick KA et al. (2016). The increasing importance of atmospheric demand for ecosystem water and carbon fluxes. Nature Climate Change 6: 1023.

Oishi AC, Hawthorne DA, Oren R (2016) Baseliner: an open-source, interactive tool for processing sap flux data from thermal dissipation probes. SoftwareX 5: 139-143.

Okamoto M, Tanaka Y, Abrams SR, Kamiya Y, Seki M, Nambara E (2009) High humidity induces abscisic acid 8 ‘- hydroxylase in stomata and vasculature to regulate local and systemic abscisic acid responses in arabidopsis. Plant Physiology 149L: 825–834.

Oren R, Sperry JS, Katul GG, Pataki DE, Ewers BE, Phillips N, Schäfer KVR (1999) Survey and synthesis of intra-and interspecific variation in stomatal sensitivity to vapour pressure deficit. Plant, Cell & Environment 22 : 1515-1526.

Poyatos R, Martínez-Vilalta J, Čermák J, Ceulemans R. Granier A, Irvine J, Köstner B, Lagergren F, Meiresonne L, Nadezhdina N, Zimmermann R, Llorens P, Mencuccini M (2007) Plasticity in hydraulic architecture of Scots pine across Eurasia. Oecologia 153 : 245–259.

Poyatos R, Granda V, Molowny-Horas R, Mencuccini M, Steppe K, Martínez-Vilalta J (2016) SAPFLUXNET: towards a global database of sap flow measurements. Tree Physiology 36: 1449-1455.

R Core Team (2015) R: A language and environment for statistical computing. R Foundation for Statistical Computing, Vienna, Austria. URL http://www.R-project.org/.

Reich PB, Walters MB, Ellsworth DS (1997) From tropics to tundra: global convergence in plant functioning. Proc Natl Acad Sci USA 94: 13730–13734

Reich PB (2014) The world-wide ‘fast–slow’plant economics spectrum: a traits manifesto. Journal of Ecology 102: 275-301.

Richards PW (1952) The tropical rain forest; an ecological study. At The University Press; Cambridge.

Schachtman DP, Goodger JQ (2008) Chemical root to shoot signaling under drought. Trends in plant science 13: 281-287.

Schlesinger WH, Jasechko S (2014) Transpiration in the global water cycle. Agricultural and Forest Meteorology 189: 115-117.

Schulze E-D, Lange OL, Buschbom U, Kappen L, Evenari M (1972) Stomatal responses to changes in humidity in plants growing in the desert. Planta 108: 259–270.

Slot M, Winter K (2017) In situ temperature response of photosynthesis of 42 tree and liana species in the canopy of two Panamanian lowland tropical forests with contrasting rainfall regimes. New Phytologist 214: 1103-1117.

Stahl C, Burban B, Wagner F, Goret JY, Bompy F, Bonal D (2013a) Influence of Seasonal Variations in Soil Water Availability on Gas Exchange of Tropical Canopy Trees. Biotropica 45: 155-164.

Stahl C, Hérault B, Rossi V, Burban B, Bréchet C, Bonal D (2013b) Depth of soil water uptake by tropical rainforest trees during dry periods: does tree dimension matter? Oecologia 173: 1191-1201.

Steppe K, De Pauw DJ, Doody TM, Teskey RO (2010) A comparison of sap flux density using thermal dissipation, heat pulse velocity and heat field deformation methods. Agricultural and Forest Meteorology 150: 1046-1056.

Swenson NG et al. (2017) Tree co-occurrence and transcriptomic response to drought. Nature communications 8: 1996.

Togashi HF et al. (2015) Morphological and moisture availability controls of the leaf area- to-sapwood area ratio: analysis of measurements on Australian trees. Ecology & Evolution 5: 1263-1270.

Torre S, Fjeld T (2001) Water loss and postharvest characteristics of cut roses grown at high or moderate relative air humidity. Scientia Horticulturae 89: 217–226.

Torre S, Fjeld T, Gislerød HR, Moe R (2003) Leaf anatomy and stomatal morphology of greenhouse roses grown at moderate or high air humidity. Journal of the American Society for Horticultural Science 128: 598–602.

van der Sande MT et al. (2016) Old-growth Neotropical forests are shifting in species and trait composition. Ecological Monographs 86: 228-243.

Whitehead D, Okali DUU, Fasehun FE (1981) Stomatalresponse to environmental variables in two tropical forestspecies during the dry season in Nigeria. Journal of Applied Ecology 18: 571–587.

Wolf A, Anderegg WR, Pacala SW (2016) Optimal stomatal behavior with competition for water and risk of hydraulic impairment. Proceedings of the National Academy of Sciences 113: E7222-E7230.

Wood PJ, Hannah DM, Sadler JP (Eds.) (2008) Hydroecology and ecohydrology: past, present and future. John Wiley & Sons.

Wright IJ et al. (2004) The worldwide leaf economics spectrum. Nature 428: 821–827.

Wright IJ et al. (2005) Modulation of leaf economic traits and trait relationships byclimate. Glob. Ecol. Biogeogr. 14: 411–421.

Wright IJ et al. (2007) Relationships Among Ecologically Important Dimensions of Plant Trait Variation in Seven Neotropical Forests. Annals of Botany 99: 1003-1015.

Xu X, Medvigy D, Powers JS, Becknell JM, Guan K (2016) Diversity in plant hydraulic traits explains seasonal and inter-annual variations of vegetation dynamics in seasonally dry tropical forests. New Phytologist 212: 80-95.

Zemp DC, Schleussner CF, Barbosa HMJ, Van der Ent RJ, Donges JF, Heinke J, Sampaio G, Rammig A (2014) On the importance of cascading moisture recycling in South America. Atmospheric Chemistry and Physics 14: 13337-13359.

Zhang K, Kimball JS, Nemani RR, Running SW, Hong Y, Gourley JJ, Yu Z (2015) Vegetation greening and climate change promote multidecadal rises of global land evapotranspiration. Sci. Rep. 5: doi:10.1038/srep15956.

Zhu SD, Song JJ, Li RH, Ye Q (2013) Plant hydraulics and photosynthesis of 34 woody species from different successional stages of subtropical forests. Plant Cell Environ 36: 879-891.

Ziemińska K, Westoby M, Wright IJ (2015) Broad Anatomical Variation within a Narrow Wood Density Range—A Study of Twig Wood across 69 Australian Angiosperms. PLoS ONE 10: e0124892.

Table 1: Characteristics of the study sites

Site code	**PNM**	**MAN**	**BCI**	**FRG**	**SLZ**	**SAB**	**SOL**
Country	Panama	Brazil	Panama	French Guiana	Panama	Puerto Rico	Costa Rica
MAT (°C), MAP* (mm)*	26, 1826	27, 2200	26, 2640	26, 3102	25, 3286	24, 3500	24, 4200
P_{DRY}* *(mm)*	53	95	60	72	70	90	100
Topography	Light slope	Flat	Flat	Light slope	Steep	Light slope	Steep
Soil depth (m)	> 6	> 20	NA	> 15	> 3	> 20	1.5
Elevation (m)	30	100	170	40	130	130	540
*Mean LAI** (m^2 m^{-2})	NA	6.0	6	6.7	NA	6.47	3.32
Soil type	Mollisol	Latosol	Oxisol	Acrisols	Oxisol	Ultisol	Andisol
*MET station (m)**	25	50	48	56	52	2	42
Sap flux method	TD	HR	TD	TD	HR	TD*	TD
Duration of the measurements (months)	12	2-5	16	24	13	12	21
References	Slot & Winter, 2017	Luizão *et al*., 2004	Detto *et al*., 2018	Bonal *et al*., 2008	Slot & Winter, 2017	Kimball *et al*., 2018	Aparecido *et al*., 2016

*_MAP_, mean annual sum of precipitation (1950-2010); *MAT*, mean annual temperature (1950-2010); P_{DRY}, *mean monthly sum of precipitation during the dry season; LAI*, leaf area index; HR, heat-ratio method; TD, thermal dissipation method; *MET station*, height of the meteorological station (m).

Table 2: Characteristics of the study trees (± SE).

Site	**Number of measured trees**	**Mean tree height (m)**	**Mean *DBH** (cm)**	**Number of target species**
PNM	4	30.7 ± 2.7	83.9 ± 18.9	4
MAN	4	32.2 ± 1.5	59.9 ± 9.6	4
BCI	6	26.6 ± 2.0	47.3 ± 6.7	5
FRG	5	27.8 ± 2.1	40.3 ± 10.9	5
SLZ	6	28.1 ± 1.5	49.9 ± 4.5	6
SAB	9	23.4 ± 0.9	28.8 ± 1.8	8
SOL	8	30.1 ± 1.1	96.7 ± 24.5	4

**DBH* = diameter at breast height

Figure legends

Figure 1: Theoretical variation in sap flux velocity (v) response to VPD: under low VPD conditions, v increases linearly with rising VPD until v reaches a saturation rate (v_{max}, grey circle) at a given VPD threshold (VPD_{max}, grey arrow). As VPD progressively increases v will either level-off at a maximum rate or start dropping progressively. Differences in v responses to increasing VPD between trees (highlighted by different dotted and bold lines) emerge from long-term adjustments to local moisture conditions (i.e. reflecting differences in foliar and wood hydraulic properties), with reductions in moisture expected to result in lower VPD_{max} and v_{max}.

Figure 2: Sub-hourly sap flux velocity (v, cm h^{-1}) as a function of vapor pressure deficit (VPD, kPa) for each site. Sites are organized going from the driest (b) to the wettest (h) (i.e. in terms of *MAP*). Dashed lines represent fitted curves using local regression function for each individual tree.

Figure 3: Relationships between the VPD threshold at which sap flux levels-off at maximum levels (VPD_{max} ± SD, kPa) and maximum sap flux (v_{max} ± SD, cm h^{-1}), and mean annual precipitation (*MAP*, mm) (panels a and c) or monthly precipitation during the dry season (P_{DRY}, mm) (panels b and d). Asterisks, situated next to the r^2 values, denote the significance of the relationships (* $P < 0.05$, ** $P < 0.01$, *** $P < 0.001$).

Figure 4: Relationships between VPD threshold at which sap flux levels-off at maximum levels (VPD_{max}, kPa) and maximum sap flux (v_{max}, cm h^{-1}), and wood specific gravity (*WSG*, g cm^{-3}) (panels a and c) or leaf mass per area (*LMA*, g m^{-2}) (panels b and c), across all sites. Each point represents a different individual tree.

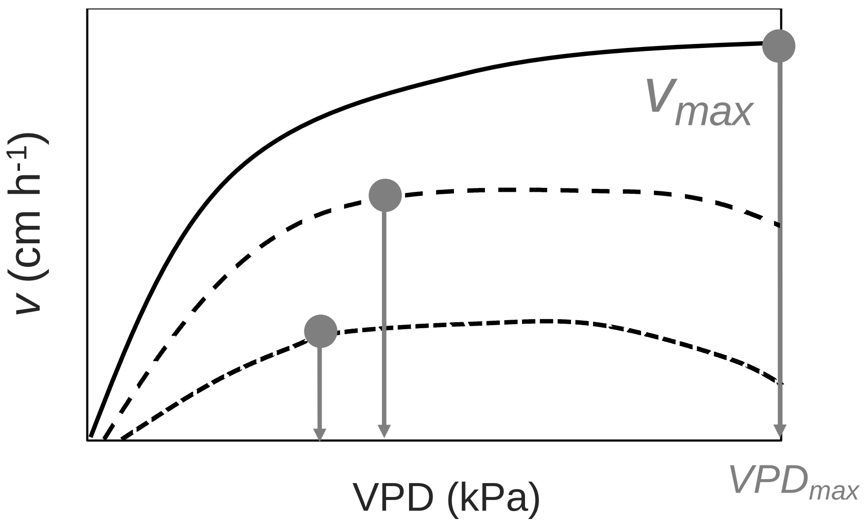

Figure 1

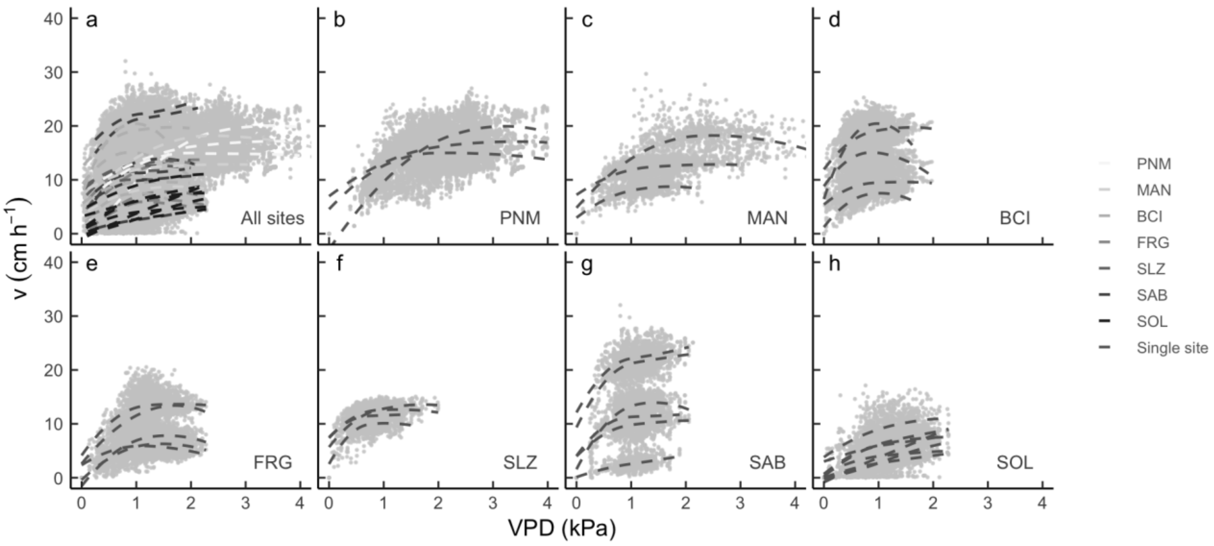

739

740

741 **Figure 2**

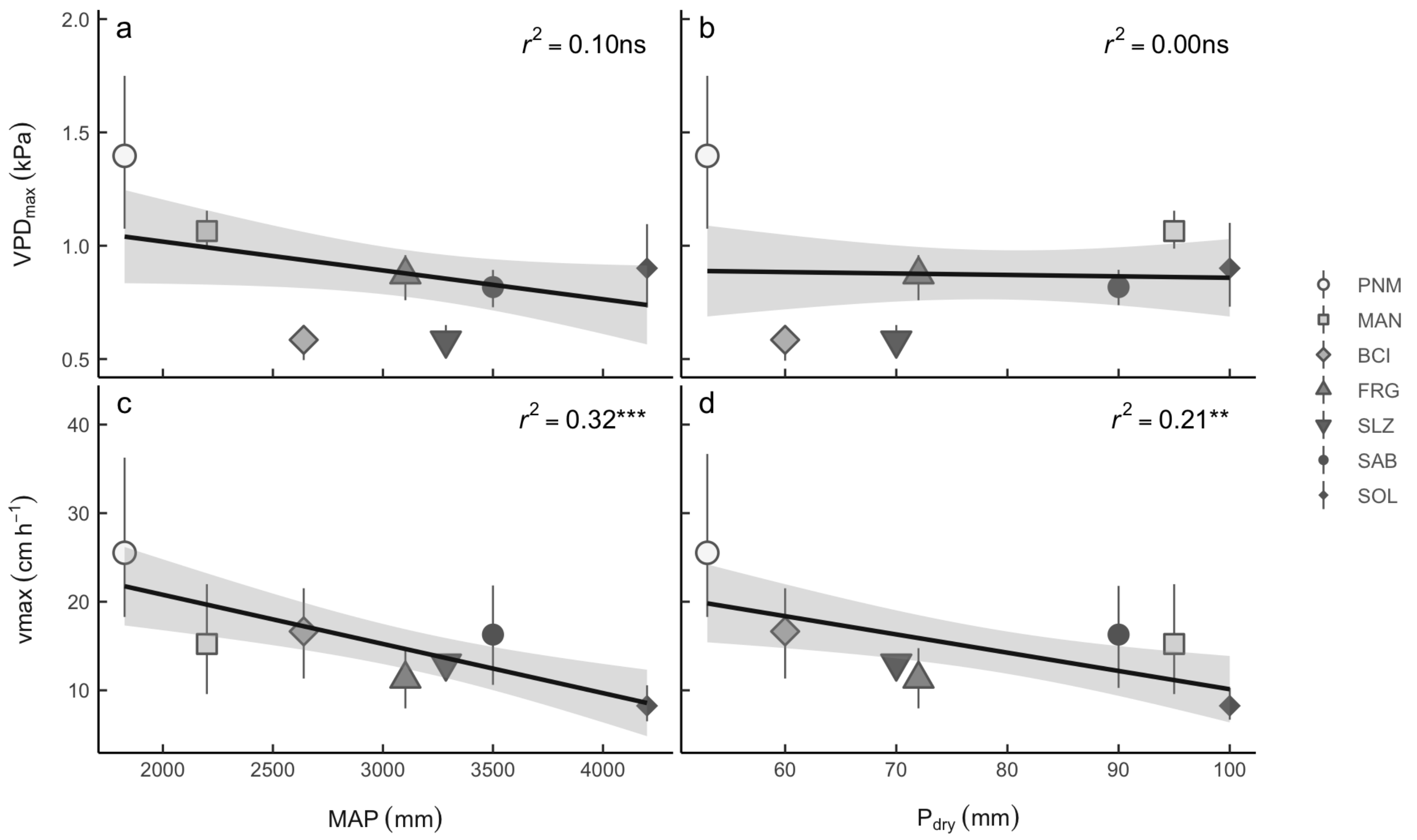
a
$r^2 = 0.10$ns
b
$r^2 = 0.00$ns
c
$r^2 = 0.32$***
d
$r^2 = 0.21$**
VPD$_{max}$ (kPa)
vmax (cm h^{-1})
2.0
1.5
1.0
0.5
40
30
20
10
2000
2500
3000
3500
4000
60
70
80
90
100
MAP (mm)
P$_{dry}$ (mm)
PNM
MAN
BCI
FRG
SLZ
SAB
SOL

Figure 3

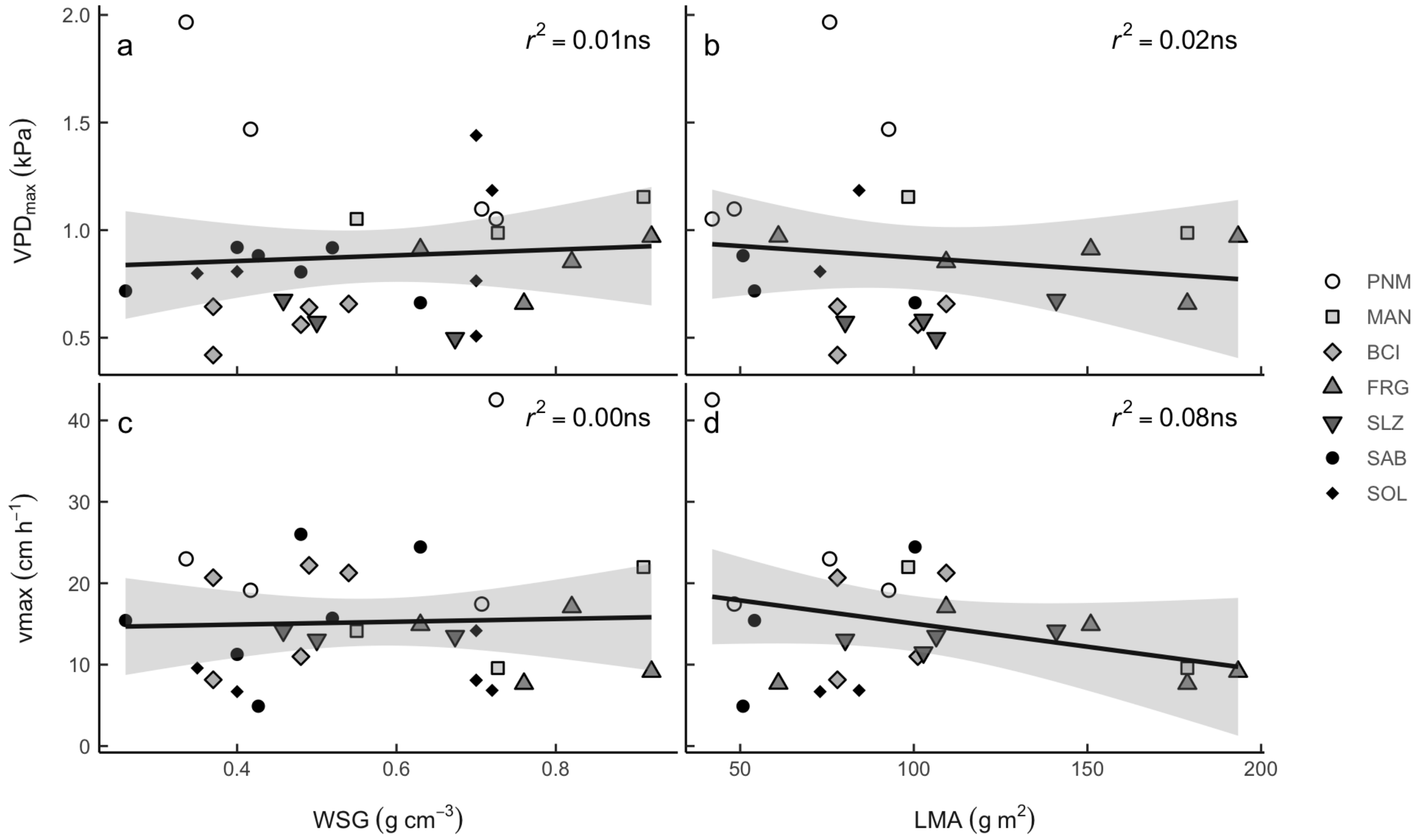a
r^2 = 0.01ns
b
r^2 = 0.02ns
c
r^2 = 0.00ns
d
r^2 = 0.08ns
VPD$_{max}$ (kPa)
2.0
1.5
1.0
0.5
vmax (cm h^{-1})
40
30
20
10
0
0.4
0.6
0.8
50
100
150
200
WSG (g cm^{-3})
LMA (g m^2)
PNM
MAN
BCI
FRG
SLZ
SAB
SOL

Figure 4